VETOR

Structural Dimensioning of an Equipment to Sinter Refuse of Recycled PET☆

Dimensionamento Estrutural de um Equipamento para Sinterização de Chapas de Refugo de PET Reciclado

Gabriel Angelo Santos Mendes†, Alexandre da Silva Scari

Department of Mechanical Engineering, Federal University of Minas Gerais, Belo Horizonte, MG, Brazil
†**Corresponding author:** gasm2016@ufmg.br

Abstract

The consumption of polyethylene terephthalate (PET) has been increasing every year, as well as its recycling process as the applications of recycled PET are diversified. However, the recycling companies are not able to recycle 100% of PET because the particles with low granulometry (refuse) are not utilized because they stick to the extruder screw and are discarded. This study presents the structural dimensioning of a proposal of an equipment to sinter this refuse in some predetermined geometries, in order to achieve possible commercial applications. This structural dimensioning was done with finite element analysis open-source software Salome Meca. Some structural modifications required to achieve the design requirements are presented. Yet, the hydraulic system to operate the compression was also dimensioned.

Keywords

Polyethylene terephthalate (PET) • Sintering • Structural dimensioning • Finite element analysis • Hydraulic system

Resumo

O consumo de polietileno tereftalato (PET) vem aumentando a cada ano, bem como sua reciclagem, pois as aplicações do PET reciclado são bem diversificadas. Entretanto, as empresas de reciclagem ainda não conseguem reciclar 100% do PET que recebem porque as partículas com granulometria muito pequena (refugo) aderem ao parafuso das extrusoras de plástico, e são descartadas. Este trabalho apresenta o dimensionamento estrutural de uma proposta de equipamento para sinterizar este refugo em geometrias pré-determinadas, a fim de atingir possíveis aplicações comerciais O dimensionamento estrutural foi feito a partir de simulações computacionais pelo método dos elementos finitos, utilizando o software Salome Meca. São apresentadas as modificações estruturais feitas para atender os requisitos do projeto. Ainda, foi feito o dimensionamento do sistema hidráulico para acionamento do sistema de compressão.

☆ This article is an extended version of the work presented at the Joint XXIV ENMC National Meeting on Computational Modelling and XII ECTM Meeting on Science and Technology of Materials, held in webinar mode, from October 13th to 15th, 2021.

Palavras-chave

Polietileno tereftalato (PET) • Sinterização • Dimensionamento estrutural • Análise por elementos finitos • Sistema Hidráulico

1 Introduction

The consumption of polyethylene terephthalate (PET) has been increasing every year. 840000 tons were consumed in Brazil in 2016. In the same way, PET recycling is increasing and its applications are quite diverse [1], as: duvet, comforters and sweatshirts; clothesline ropes and brooms; rulers, clocks, pencil holders and pens; water tanks, pipes and connections, faucets, swimming pools; tiles, synthetic marble; paints and varnishes, automotive industry. However, the recycling companies are not able to recycle 100% of PET because the particles with low granulometry (refuse) are not utilized because they stick to the extruder screw and are discarded. For example, a PET recycling company located in Juiz de Fora-MG, Brazil, produces an average of 700 kg of refuse recycled PET [2].

The recycling of polyethylene terephthalate (PET) and its application has been the target of many researches, most of all by extrusion [3-7].

The sintering process consists of compacting and heating a particulate material simultaneously, forming a solid body and often with good mechanical strength [8]. Concerning the recycled PET refuse sintering, it is possible to do it in a press for metallographic samples, but the geometry obtained is a disk with 40 mm of diameter and an average height of 18 mm [2]. Its mechanical properties were evaluated, testing different values of pressure and sintering temperature, and performed some compression tests with these specimens [9]. Also, the optimum sintering parameters of recycled PET refuse were determined along with its mechanical and machining properties by compression tests and drilling (with a bench drill) and manual sawing (with a saw frame) [10]. These three researchers demonstrated that the final product obtained by the recycled PET refuse sintering has potential to commercial applications as drywall and furniture. Therefore, it is necessary to sinter in a rectangular format, and there is no equipment on the market for this purpose by now.

This being said, the goal of this study is to present a proposal of such an equipment. The structural dimensioning along with its hydraulic system are detailed below.

2 Materials and methods

Table 1 presents the design requirements.

Table 1: Design requirements.

Requirement	Value	Unit
Rectangular plate dimensions	1000 x 600 x 20	mm
Sintering pressure	50	kgf/cm^2

The initial conception of this equipment was based on benchmarking of commercial presses of four columns. First of all, a conception of this equipment was done with the open-source software FreeCAD. Figure 1 shows the 3D model of its conception where the four principal substructures designed in this work are indicated: the upper structure, the press plate, the lower structure and the press box, in addition to the clamping columns and the hydraulic actuator cylinder.

The ASTM A36 steel was the first option for the structure due to its low cost and good mechanical strength. However, later the ASTM A572 steel was considered as it presents a similar cost as ASTM A36 steel but with better mechanical strength. This allowed the specification of thinner steel plates and consequently less final weight.

The maximum allowable stress and the maximum allowable displacement for this structural design was defined according to [11]. Table 2 presents the mechanical properties of ASTM A572 and ASTM A36 steels, as well as the safety factors for this design.

Table 2: Mechanical properties of ASTM A572 and ASTM A36 steels, and the safety factors defined.

Parameter	ASTM A36	ASTM A572
Elasticity modulus	200 GPa	200 GPa
Poisson	0,3	0,3
Yield stress	250 MPa	345 MPa
Ultimate stress	350 MPa	450 MPa
Density	7850 kg/m^3	7850 kg/m^3
Safety factor	1,2	1,2
Allowable maximum stress	208,3 MPa	287,5 MPa
Allowable maximum displacement	1 mm	1 mm

The structures were design by finite element analysis with the open-source softwares Salome Meca and Code Aster solver. In order to reduce the manufacturing costs of this equipment, it was defined steel plate thickness up to 25,4 mm. Thicker steel plates were adopted only where there was no choice. Various geometry concepts were evaluated until an appropriate proposal was defined according to the design requirements.

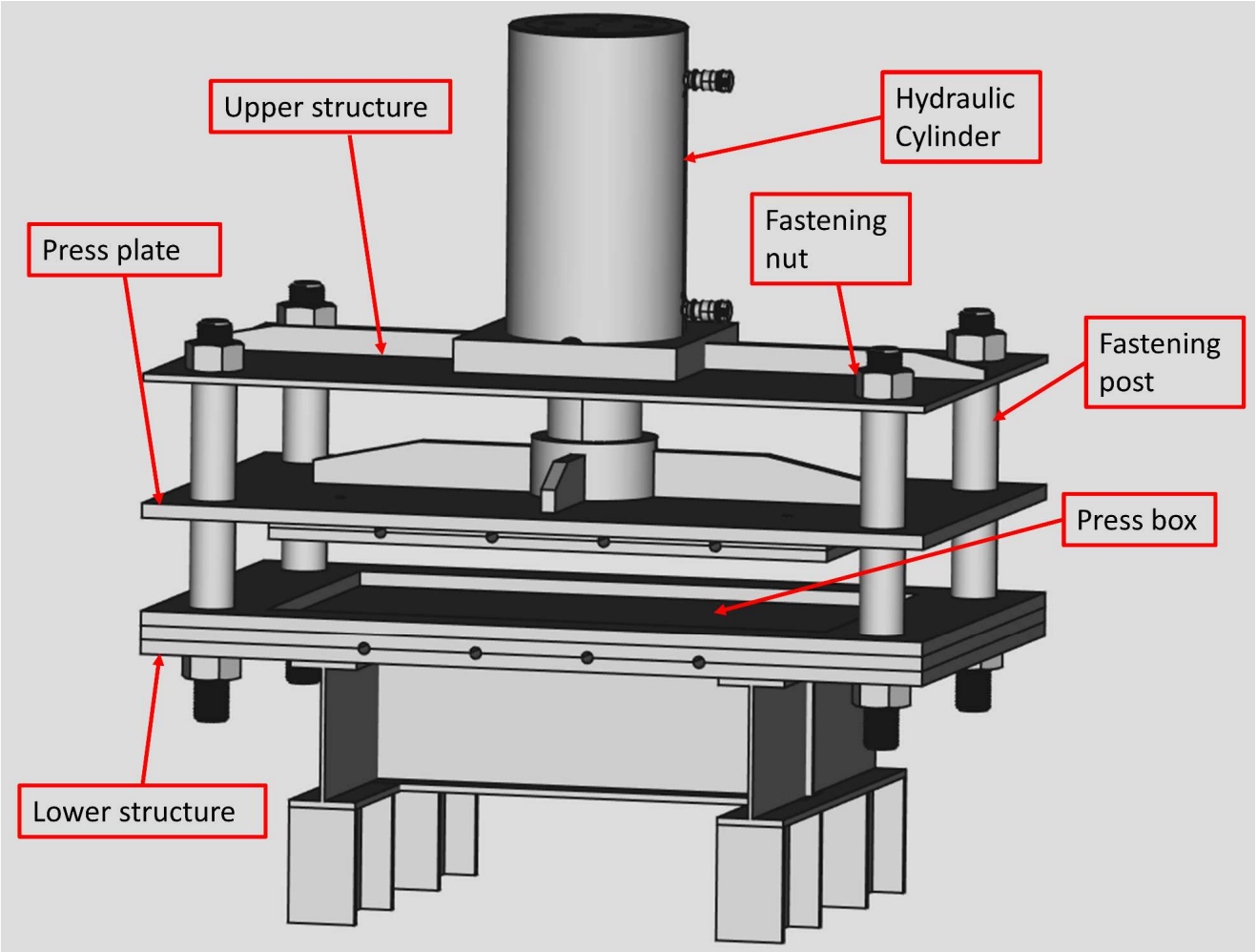

Figure 1: Initial concept of the equipment.

For the compression system, both power screws and hydraulic cylinders were considered. The option for the hydraulic cylinder is due to its better maintenance, safety and also based on the recommendations by Fialho (2006) for hydraulic systems.

The design of the four substructures is presented in the next sections, along with the dimensioning of the hydraulic system.

2.1 Upper structure dimensioning

The Upper structure must stand the reaction force of the hydraulic cylinder (300 tf), so it is mainly subject to bending. Initially it was designed with a 1400x800x25.4 mm steel plate with reinforcements along its length and a hole in its intermediate portion where the hydraulic cylinder will be fixed. These steel plates were modeled with shell quadrilateral elements of 20 mm, and a mesh refinement in the hole region (element size = 5 mm). The cylinder reaction force (300 tf) was distributed among the nodes of the inner part of the central hole. Figure 2 shows the finite element model of the Upper structure where it is possible to see the mesh and its refinement, along with the nodes subjected to the load.

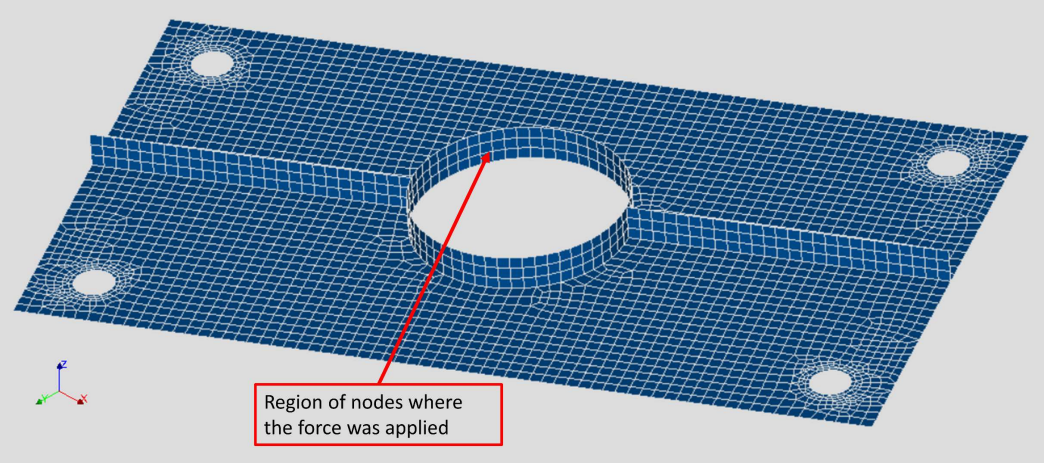

Figure 2 : Initial finite element model of the upper structure.

The boundary conditions were applied in the contact region with the nuts: displacement in the Z direction was restricted, along with the three directions in the inner part of the hole as they keep in touch with the columns (see Fig. 3).

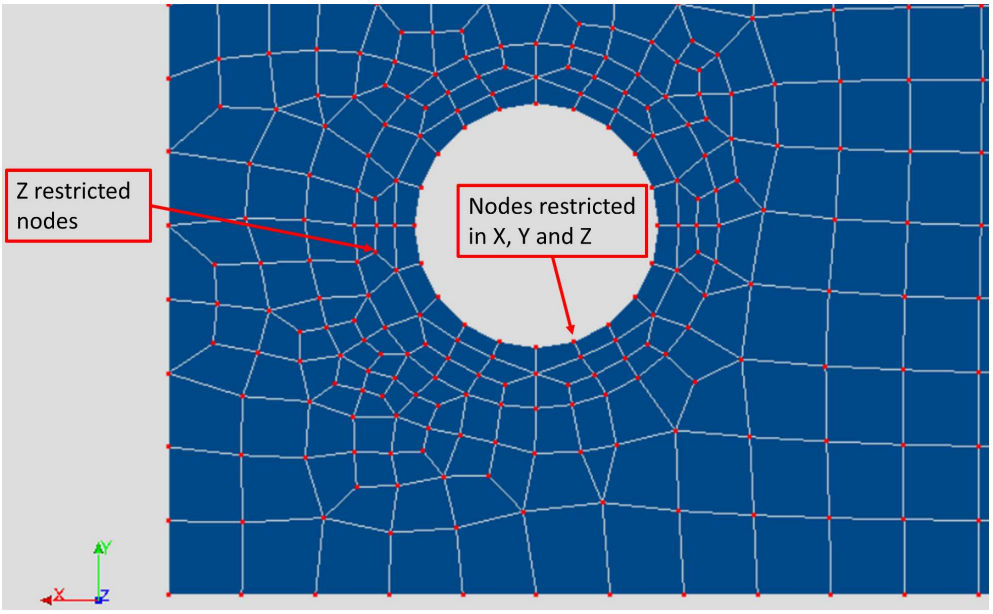

Figure 3: Displacement constraints of the upper structure finite element model.

2.2 Press plate dimensioning

The press plate transmits the compression force from the hydraulic cylinder to the sintering material. It should also support the heating electrical resistances as it has holes in its underside. The initial plate dimensions were 1000x600x25.4 mm with four reinforcements in its top side. It was modeled with solid tetrahedral elements of 20 mm in size, and a mesh refinement in the hole region (element size = 5 mm). The reaction force of the hydraulic cylinder was applied in the upper region of the round beam.
Figure 4 shows the finite element model of the press plate.

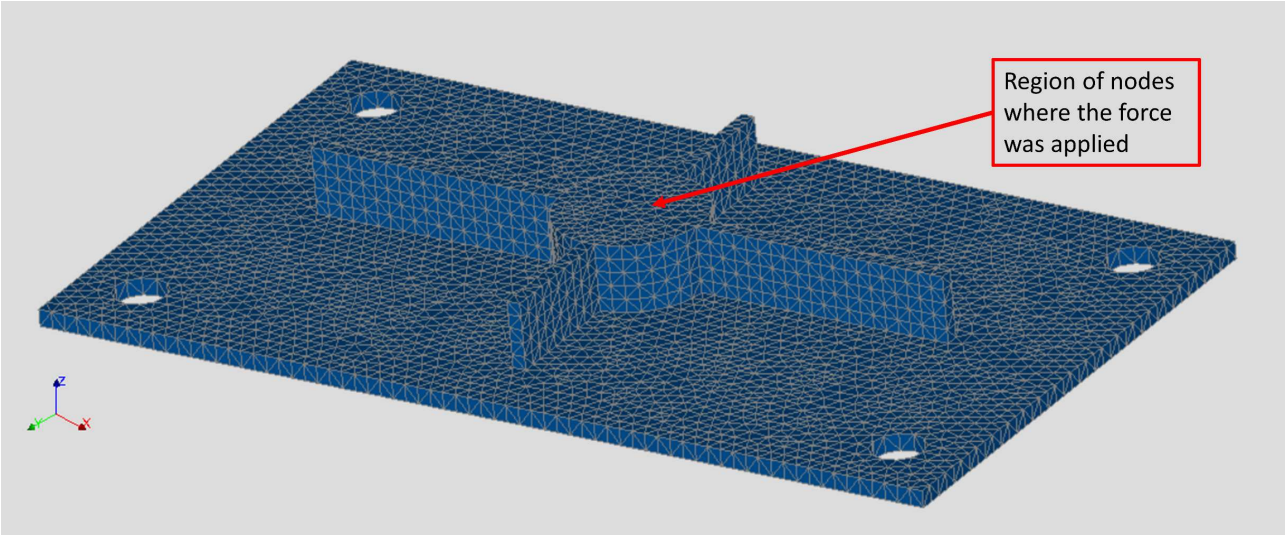

Figure 4: Initial finite element model of the press plate.

The displacements were applied in the lower side where there is contact between the two symmetric plates. The *X*, *Y* and *Z* displacements of the external lateral nodes were restricted because they have contact with the lateral walls of the press box where the recycled PET refuse will be placed, while the inner nodes were restricted only in the *Z* direction (see Fig. 5).

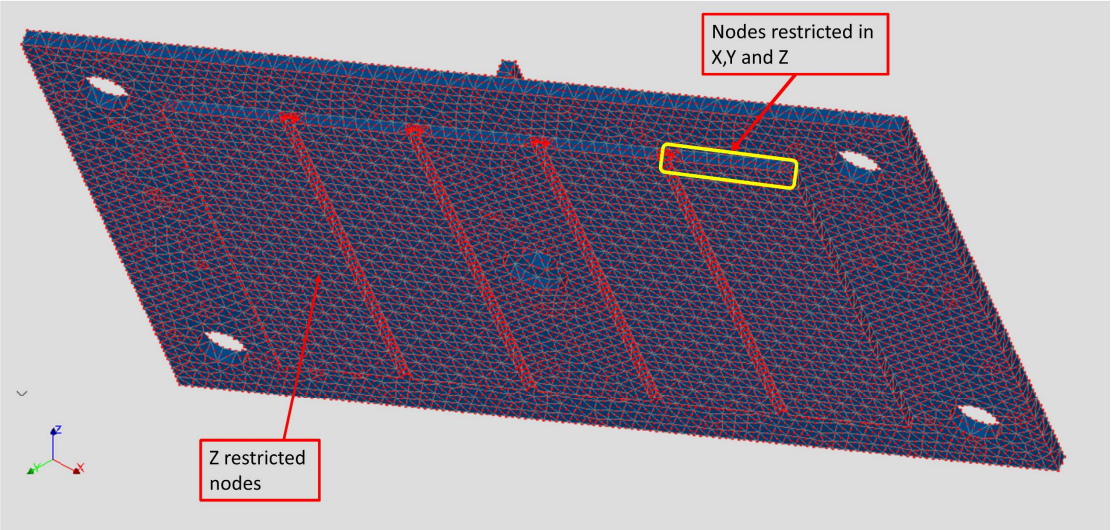

Figure 5: Displacement restrictions for the press plate.

2.3 Lower structure dimensioning

The lower structure must stand the box where the recycled PET refuse will be placed during the sintering process, as it must withstand the compression force from the hydraulic cylinder, that will end up in bending similar to the upper structure. Initially, it was designed as only a plate of dimensions: 1400 x 800 x 25.4 mm, with four holes to the mount the columns. However, the lower structure was calculated after the upper and the expected results were known: the structure had no enough inertia to withstand the loads. So, the lower structure model was designed as a box girder in order to improve the inertia and thus withstand the loads. It was modeled with shell quadrilateral elements of 20 mm in size, and a mesh refinement in the hole region (element size = 5 mm). The load was applied in the region of the press plate. Figure 6 shows the finite element model of the lower structure.

The restrictions applied were similar to the upper structure. The displacements of the nodes in contact with the nuts were restricted in Z and the ones on the inner side of the hole, in both X and Y directions (see Fig. 7).

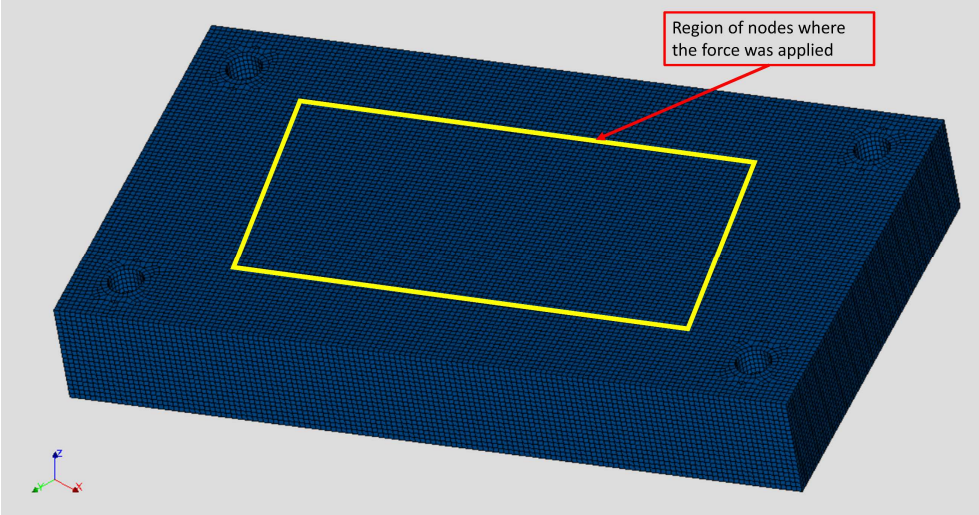

Figure 6: Lower structure.

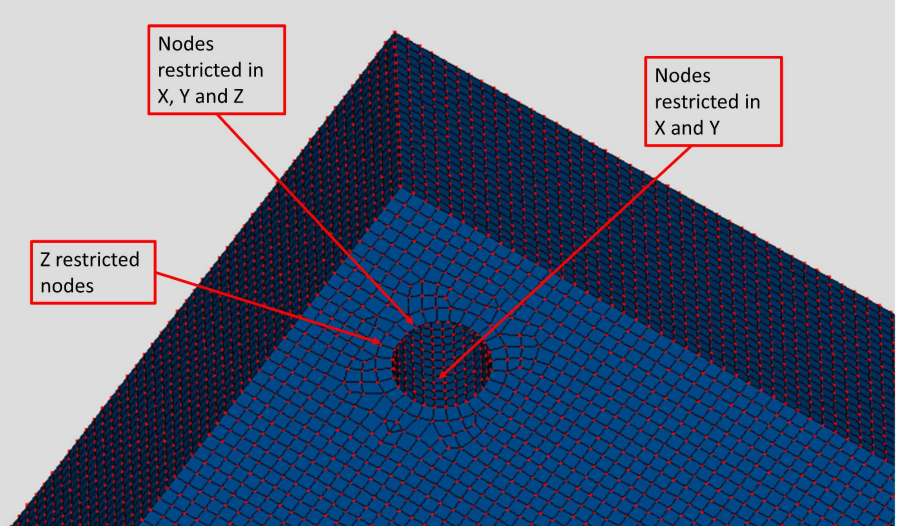

Figure 7: Lower structure restrictions.

2.4 Press box dimensioning

The press box is where the recycled PET refuse will be placed during the sintering process and thus must withstand the compression force upon it. Its first design had only a plate with an undercut with the dimensions of the final

sintered product. But, due to some manufacturing complications and to the lower structure modifications, its design was modified to five plates as an open box. It was modeled with shell quadrilateral elements of 20 mm (see Fig. 8).

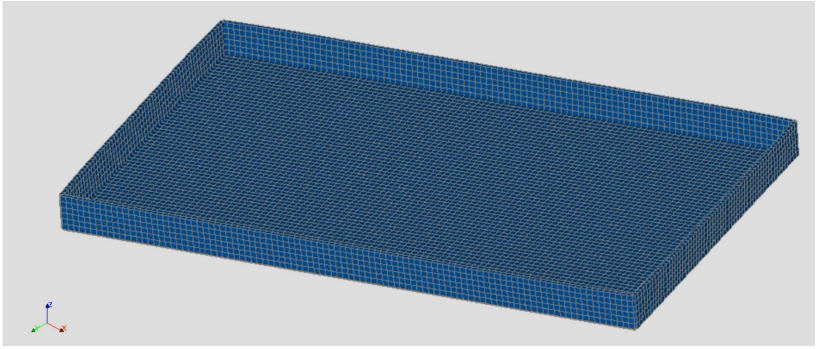

Figure 8: Press box.

The load was applied on the lateral plate nodes and, the restrictions, on the lower plate nodes (see Fig. 9).

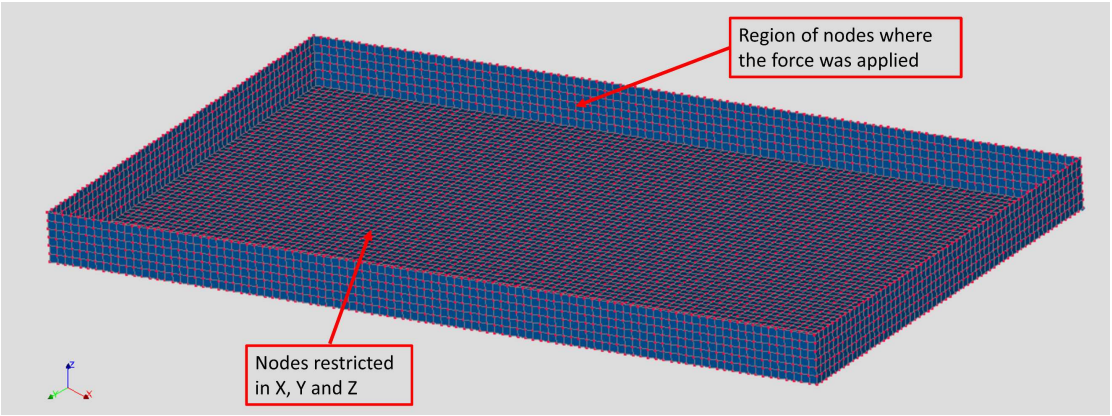

Figure 9: Boundary conditions for the press box.

2.5 Hydraulic dimensioning

Considering the pressure required to press the superficial area of the final sintered plate, the hydraulic cylinder actuating force was determined and, thus, a commercial hydraulic cylinder was specified. Then, it was necessary to design the hydraulic circuit, starting with the hydraulic pump. The required pressures for the forward and return of the hydraulic cylinder were determined with Eqs. (1) and (2).

$$P_a = \frac{F_a}{A_{efa}}. \tag{1}$$

$$P_r = \frac{F_r}{A_{efr}}. \tag{2}$$

Where P_a, P_r, F_a, F_r, A_{efa} and A_{efr} are the admission pressure, the required force and the net area of the cylinder for its forward and return. The nominal pressure of the hydraulic pump is higher than forward pressure. However, when specifying the hydraulic pump, it was necessary to verify the total time for the forward and return of the cylinder considering the hydraulic pump flow rates, with Eqs. (3) and (4).

$$t_a = \frac{Cap_a}{Q_B}. \tag{3}$$

$$t_r = \frac{Cap_r}{Q_B}. \tag{4}$$

Where t_a and t_r , Cap_a and Cap_r are the time and oil capacity of the hydraulic cylinder for its forward and return.

With the hydraulic pump specified, the hydraulic piping was dimensioned. First it was necessary to determine the minimum inner diameter with Eq. (5).

$$d_{min} = \sqrt{\frac{4 \times Q_B}{\pi \times V_f}}. \tag{5}$$

Where d_{min} is the minimum pipe diameter and, V_f , the fluid velocity recommended for the required hydraulic pressure[12]. Thus, a commercial piping was selected, with its internal diameter higher than the calculated.

To verify if the fluid flow was laminar or turbulent by determining the new fluid velocity considering the commercial pipe diameter with Eq. (6) and obtaining the Reynolds number with Eq. (7).

$$V_f = \frac{4 \times Q_B}{\pi \times d_t^2} \tag{6}$$

$$Re = \frac{V_{f2} \times d_t}{\gamma} \tag{7}$$

Where Re is the Reynolds number, V_{f2} the new fluid velocity, and γ the a kinematic viscosity of the working fluid.

Finally, the minimum hydraulic fluid reservoir volume with the Eq. (8) [12].

$$V_{min} = 3 \times Q_B \tag{8}$$

Where V_{min} is the minimum hydraulic fluid reservoir volume (in liters), and Q_B is the hydraulic pump flow rate (liters per minute).

3 Results

3.1 Upper structure dimensioning

Figure 10 shows the von Mises stress obtained by the finite element analysis (FEA) for the upper structure. Its maximum value is higher than the allowable stress of 208.33 MPa in many regions, with values up to 10.000 MPa, and the maximum displacement obtained is 86 mm, which shows that this structure was undersized.

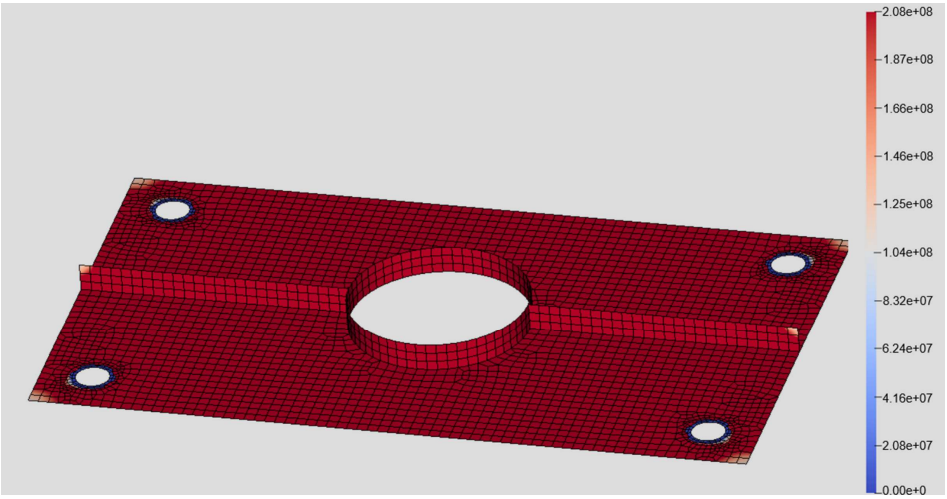

Figure 10: FEA results for the Upper structure.

So, many geometries were evaluated. Figure 11 presents the intermediate geometry for this structure where it was defined a box girder geometry in order to increase its inertia. However, it was not very effective as the maximum von Mises stress was up to 500 MPa with 2.2 mm displacement.

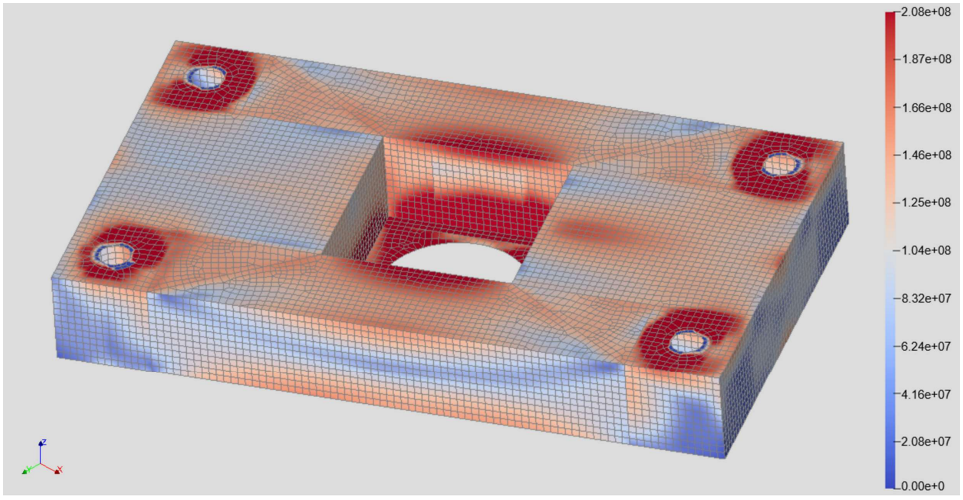

Figure 11: FEA results for the intermediate upper structure geometry.

New geometries were evaluated until the final one presented in Fig. 12 where the cylinder fixation region was modified with the addition of another structure to hold it. This new geometry generated a better stress distribution along this structure. The maximum von Mises stress was up to 200 MPa only in concentration points, and the maximum displacement obtained was 0.8 mm. So, this upper structure geometry was approved.

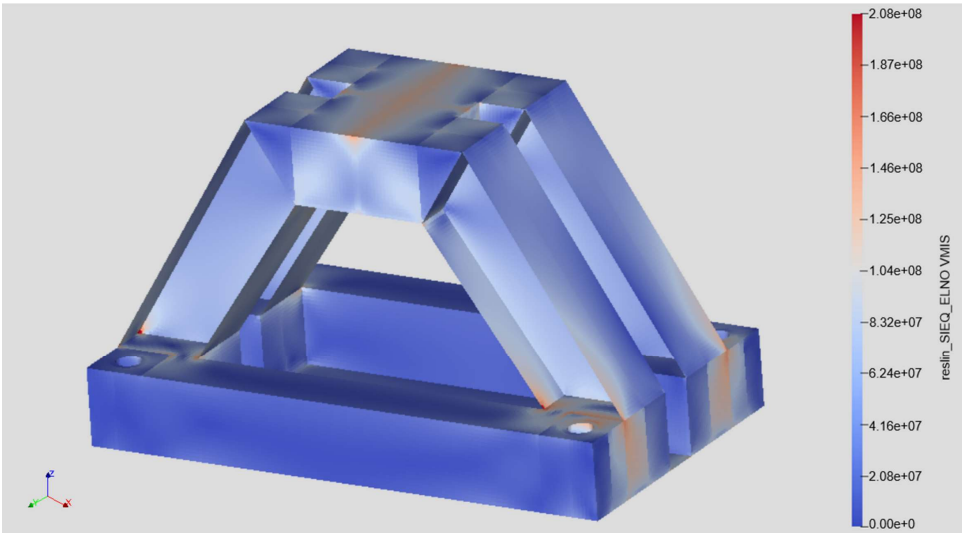

Figure 12: FEA results for the final Upper structure geometry.

3.2 Press plate dimensioning

As it is mainly under compression the actuating stress obtained was low, under 130 MPa, and the maximum displacement was 0.06 mm. In order to get a better load distribution over this plate, four new reinforcements were added (see Fig. 13) where it can be seen a better stress distribution compared to the older geometry.

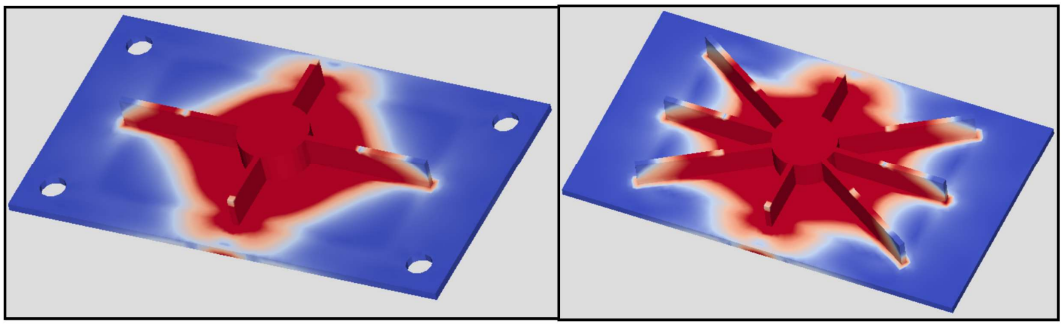

Figure 13: Stress distribution comparative for the press plate considering four new reinforcements.

3.3 Lower structure dimensioning

The maximum von Mises stress obtained was 175 MPa for the lower structure and, the maximum displacement, 1 mm. Thus, the lower structure was approved on its first proposal (see Fig. 14).

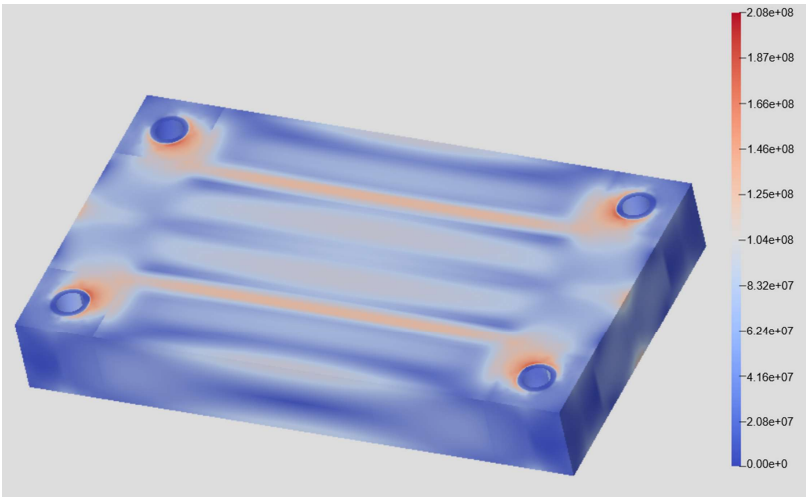

Figure 14: FEA results for the lower structure.

3.4 Press box dimensioning

The press box was initially considered with 25.4 mm in thickness but, as the maximum von Mises stress value was considerably low, thicker plates were adopted. In the end, 9.53 mm in thickness resulted in von Mises stress equal to 96 MPa with 0.08 mm in displacement (see Fig. 15).

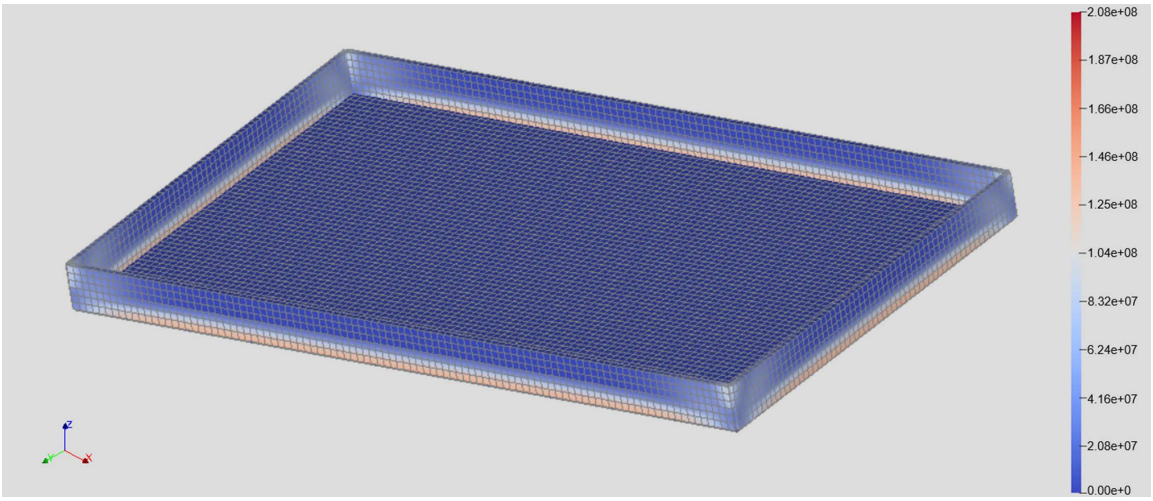

Figure 15: FEA results for the press box with 9.53 mm in thickness.

3.5 Final structural proposal for the equipment

Figure 16 shows the final structural proposal for the equipment considering all the modifications made in all the four sub-structures. Plates were included in the lower part of the equipment only for aesthetic purposes.

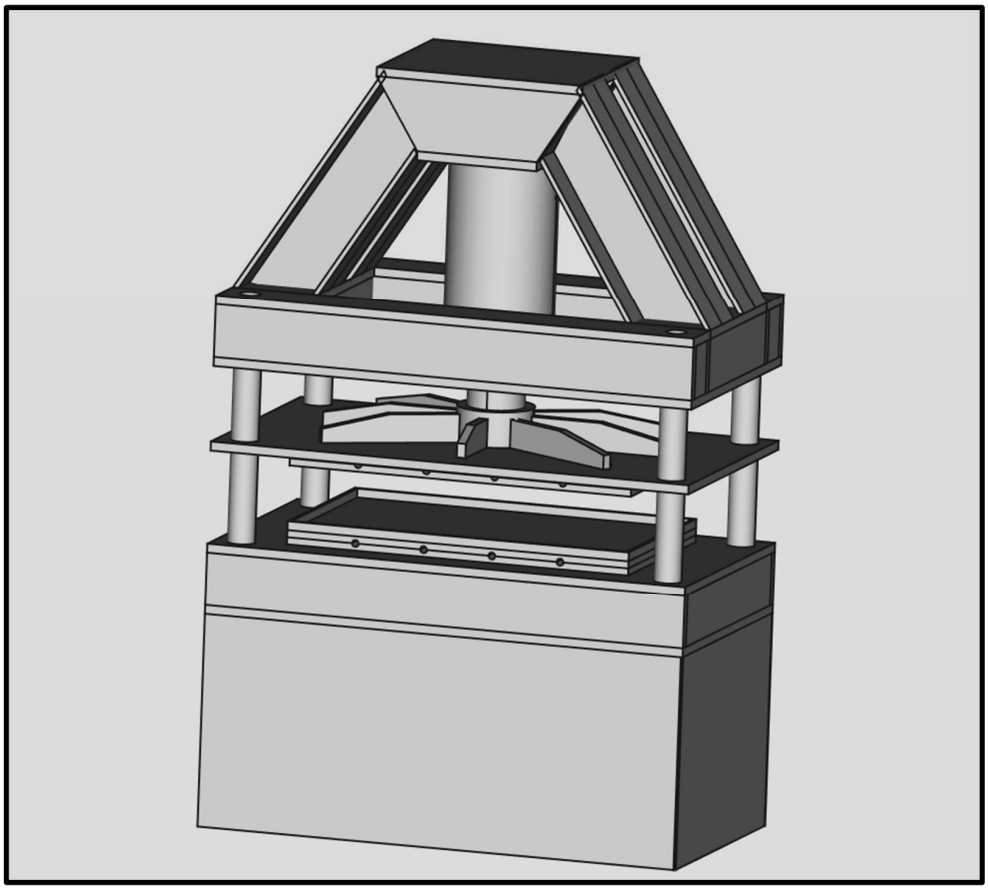

Figure 16: Final structural proposal for the equipment.

3.6 Hydraulic dimensioning

Table 3 presents the values obtained for the actuating force, required hydraulic pump pressure and the commercial items specified. It is also shown the hydraulic cylinder operating time. The hydraulic pump has two working stages: the first has low fluid rate and high pressure, required for the compression time; the second has high fluid rate and low pressure, used to allow a fast approximation of the hydraulic.

Table 3: Hydraulic pump and cylinder parameters.

Parameter	Value	Unit
Forward hydraulic cylinder required force	300	tf
Forward hydraulic cylinder oil capacity	13.9	l
Return hydraulic cylinder oil capacity	7.4	l
Forward hydraulic cylinder net area	457.3	cm^2
Return hydraulic cylinder net area	243.1	cm^2
Forward hydraulic cylinder required pressure	579	bar
Return hydraulic cylinder required pressure	0.9	bar
Hydraulic pump nominal pressure for first stage	700	bar
Hydraulic pump nominal pressure for the second stage	7	bar
Hydraulic pump volumetric flow rate - first stage	1.96	l/min
Hydraulic pump volumetric flow rate - second stage	13.9	l/min
Hydraulic cylinder forward time	59.8	s
Hydraulic cylinder return time	31.8	s

Table 4 presents the hydraulic piping dimensioning results. The fluid flow is laminar as the Reynolds number obtained is under 2000.

Table 4: Hydraulic piping dimensioning results.

Parameter	Value	Unit
Recommended fluid velocity for the work pressure	6	m/s
Minimum piping diameter for the recommended fluid velocity	3.6	mm
Pipe commercial diameter	9.7	mm
Recommended fluid velocity for the work pressure	0.4	m/s
Kinematic viscosity for the selected hydraulic fluid	32	mm^2/s
Reynolds number	134	-
Hydraulic fluid reservoir minimum volume	41.7	l

4 Conclusions

The results obtained in this work were satisfactory as commercial structure geometries were selected to withstand the equipment working conditions without the need for thicker plates, reducing its final weight and manufacturing costs.

The hydraulic dimensioning tried to consider all the parameters to allow the correct equipment working conditions, and it was possible to select commercial parts for the hydraulic system.

This innovative equipment will allow the solid PET refuse reduction, creating commercial applications for a material that is discharged nowadays.

The thermal dimensioning of this equipment is ongoing.

5 Acknowledgments

The authors would like to thank the support of the “Pró-Reitoria de Pesquisa da Universidade Federal de Minas Gerais, PRPq – UFMG”.

References

[1] ABIPET. *Brazilian PET Industry*. Available at: http://www.abipet.org.br/uploads/File/Market%20Overview%202013.pdf.

[2] W. F. Costa, *Avaliação da Viabilidade de Obtenção de Peças Densas a Partir do Processo de Prensagem a Quente de Pó de Polietileno Tereftalato (PET) Reciclado*. Bachelor thesis, Mechanical Engineering, Federal University of Juiz de Fora - UFJF, Brazil, (in Portuguese), 2016.

[3] A. F. Ávila and M. V. Duarte, “A mechanical analysis on recycled PET/HDPE composites,” *Polymer Degradation and Stability*, vol. 80, no. 2, pp. 373–382, 2003. Available at: https://doi.org/10.1016/S0141-3910(03)00025-9

[4] A. L. F. M. Giraldi, J. R. Bartoli, J. I. Velasco, and L. H. I. Mei, “Glass fibre recycled poly(ethyleneterephthalate) composites: mechanical and thermal properties,” *Polymer Testing*, vol. 24, no. 4, pp. 507-512, 2005. Available at: https://doi.org/10.1016/j.polymertesting.2004.11.011

[5] A. L. F. M. Giraldi, R. C. Jesus, and L. H. I. Mei, “The influence of extrusion variables on the interfacial adhesion and mechanical properties of recycled PET composites,” *Journal of Materials Processing Technology*, vol. 162-163, pp. 90-95, 2005. Available at: https://doi.org/10.1016/j.jmatprotec.2005.02.046

[6] R. M. Meri, J. Zicans, R. Maksimovs, T. Ivanova, M. Kalnins, R. Berzina, and G. Japins, “Elasticity and long-term behavior of recycled polyethylene terephthalate (rPET)/montmorillonite (MMT) composites,” *Composite Structures*, vol. 111, pp. 453-458, 2014. Available at: https://doi.org/10.1016/j.compstruct.2014.01.017

[7] N. E. Zander, M. Gillan, Z. Burckhard, and F. Gardea, “Recycled polypropylene blends as novel 3D printing materials,” *Additive Manufacturing*, vol. 25, pp. 122-130, 2019. Available at: https://doi.org/10.1016/j.addma.2018.11.009

[8] D. V. Shatokha, *Sintering - Methods and Products*. Rijeka: InTech, 2012.

[9] Ferreira G.A. (2017), *Avaliação das propriedades mecânicas de peças densas a partir do processo de prensagem a quente de pó de polietileno tereftalato (PET) reciclado*. Bachelor’s thesis, Mechanical Engineering, Federal University of Juiz de Fora - UFJF, Brazil, (in Portuguese), 2017.

[10] G. Cipriano Jr., *A Influência dos Parâmetros de Sinterização nas Propriedades Mecânicas do Refugo de PET*. Bachelor’s thesis, Mechanical Engineering, Federal University of Juiz de Fora - UFJF, Brazil, (in Portuguese), 2019.

[11] ABNT, Associação Brasileira de Normas Técnicas, NBR 8800:2008, *Projeto de estruturas de aço e de estruturas mistas de aço e concreto de edifícios*, Rio de Janeiro, (in Portuguese), 2008.

[12] A. B. Fialho, *Automação Hidráulica: projetos, dimensionamento e análise de circuitos*, 4th ed., São Paulo, Brazil: Érica, (in Portuguese), 2006.